Slosh Suppression by Robust Input Shaping

Brice Pridgen, Kun Bai, William Singhose
George W. Woodruff School of Mechanical Engineering
Georgia Institute of Technology
Atlanta, Georgia 30332-0405

***Abstract*— The majority of slosh-control techniques have required feedback control to suppress liquid oscillations induced by container motion. However, input shaping is an alternative method for generating motion commands that reduce residual oscillations without the need for sensors. In addition, input shaping can accommodate two concerns associated with slosh: peak transient slosh and changes in slosh frequency. Past work has demonstrated that input shaping can be useful for suppressing slosh, but none have experimentally verified robust input shapers. This paper describes simulation and experimental results that verify robust input shaping can effectively reduce peak transient slosh and limit residual oscillations over a range of parameters.**

I. Introduction

Slosh is the oscillation of liquid inside a container. There are many cases where sloshing is undesired. In the packaging and metal industries, excessive slosh can spill liquids or molten metal [30]. Sloshing of fuel and other liquids in vehicles can result in unwanted dynamics and dangerous rollovers [3]. This is especially true for space vehicles where excessive slosh can cause instability [19]. Therefore, it is often desirable to reduce peak transient slosh and residual surface oscillations induced by container motion.

There has been significant research to characterize and control slosh. A main thrust of research was driven by NASA. This work covered the governing equations, experimental results for a variety of container shapes, and the modeling of slosh in dynamic systems [2], [6], [12], [21].

In order to suppress slosh, a variety of methods have been proposed, simulated, and tested. Some techniques are passive [16], or rely on actuators near the liquid surface for slosh suppression [11], [32]. However, it is often not practical to place actuators in or near the liquid. The majority of proposed techniques use the container motion as the control input in a feedback loop. Examples of these include: sliding mode control [4], [14]; H_∞ control [30], [35]; PID control [27]; a hybrid shape approach [13], [17], [33], [34]; and iterative learning control [9]. Some control schemes filter the input to create a prescribed motion that results in minimal residual oscillation [5], [7]. Several experimental test rigs have been constructed [1], [2], [7], [8], [10], [31].

Input shaping is a control method that convolves a reference command with a series of impulses to generate a command that induces minimal residual oscillations. There have been several implementations of input shaping as a means to control slosh [1], [7], [10], [20], [29], [31]. However, no reports have shown experimental verification of input shapers that are robust to parameter variation. This paper reports simulated and experimental evaluation of robust input shaping for slosh suppression. The following sections describe the system model and testing apparatus, and then simulation and experimental results are reported.

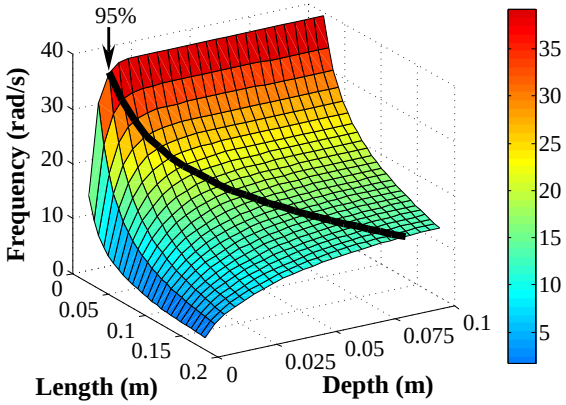

Figure 1. Slosh Frequency of Liquid Surface

II. System Modeling

A. Slosh

Using several simplifying assumptions, the natural frequency of the first mode of a liquid surface in a rectangular container can be described by [2]:

$$\omega = \sqrt{\frac{g\pi}{a}\tanh\left(\frac{h\pi}{a}\right)}, \tag{1}$$

where g is the gravitational acceleration, a is the container length in the direction of wave motion, and h is the liquid depth. A more complex equation incorporates the width dimension and can estimate higher modes. Experimental testing has shown that (1) often predicts the frequency with less than 5% error in many cases [18].

The three dimensional surface plot of slosh frequency versus container length and liquid depth is shown in Figure 1. Decreasing the container length results in a higher slosh frequency. As the liquid depth increases, the hyperbolic tangent term approaches unity and the frequency approaches a theoretical limit. As a result, the slosh frequency changes very little with depth after a critical depth. For example, the line superimposed on Figure 1 shows the liquid depths at which the slosh frequency reaches 95% of its maximum

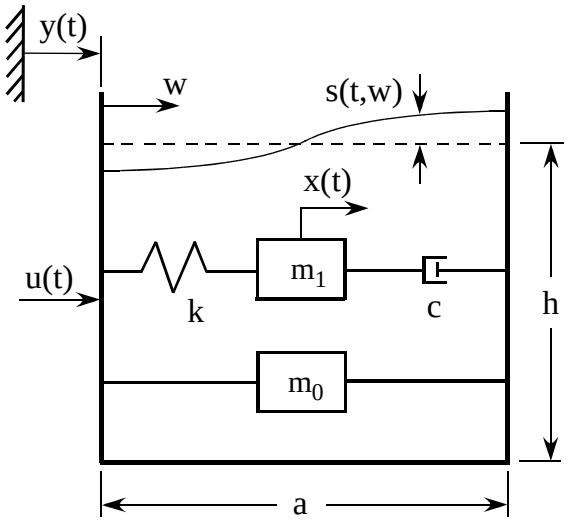

Figure 2. Slosh Model

value. This line corresponds to liquid depths that are nearly half of the container length.

Analytical expressions have also been determined for the damping ratio, showing it to be approximately 0.01 for water. The analytical expression for the damping ratio is a function of an experimentally-found constant, the Galilei number, and container geometry; however, it can have up to 25% error [18]. For this reason, the damping ratio for the tests reported here were determined experimentally.

B. Dynamic System

An open container of liquid can be approximated by the model shown in Figure 2. The force input, $u(t)$, results in container motion, $y(t)$. A damped vibratory response, $x(t)$, is modeled by a mass, spring, and dashpot. This response induces slosh on the surface, $s(t,w)$, which is a function of the measurement location, w.

This is a linearized model of the commonly-used pendulum model of slosh, and only the first mode of slosh is modeled. Here, m_1 is the mass of liquid that sloshes, and m_0 is the combined mass of the stationary liquid and the container. The spring and dashpot values are functions of the slosh frequency and damping ratio. The dimensions a and h used in (1) are also shown.

Translating the container with limited residual oscillation is desirable. But it is often also necessary to limit the peak transient slosh, to some critical value. For example, the critical value may be the height of the edge of the container. The deflection of the sloshing mass, $x(t)$, will be used to represent the surface motion at the right-most point, $s(t,a)$.

C. Input Shaping

The input-shaping process is illustrated in Figure 3. A reference step command is convolved with an input shaper containing two positive impulses. The result of the convolution is the two-step command. Note that the reference step command causes a residual vibration equal to the step

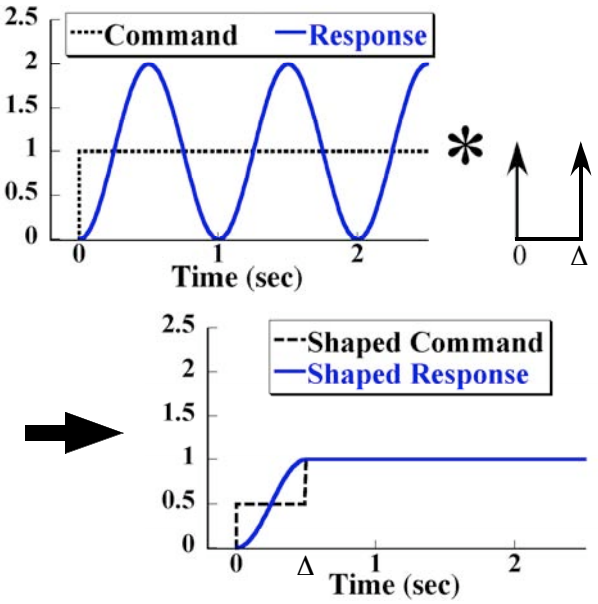

Figure 3. Input-Shaping Process

amplitude; and the input-shaped command eliminates the residual vibration [22], [23].

The key to designing an input shaper is knowledge of the system natural frequency, ω, and damping ratio, ζ. The amplitudes and time locations of the impulses in the input shaper can be found from this information. For example, the time locations and amplitudes of the shaper shown in Figure 3 are [24], [28]:

$$\begin{bmatrix} t_i \\ A_i \end{bmatrix} = \begin{bmatrix} 0 & 0.5T_d \\ \frac{1}{1+K} & \frac{K}{1+K} \end{bmatrix}, \quad i = 1,2 \tag{2}$$

where,

$$K = e^{\left(\frac{-\zeta\omega}{\sqrt{1-\zeta^2}}\right)} \tag{3}$$

and T_d is the damped period of vibration. The input shaper given in (2) produces Zero Vibration (ZV) at the design frequency. A more robust shaper is the three-impulse Zero Vibration Derivative (ZVD) input shaper. It also produces zero vibration at the design frequency, but allows for greater tolerance to modeling errors [22]:

To eliminate multiple vibration modes, additional shapers or more complex shapers are required. Specified Insensitivity (SI) shapers are generated by specifying a tolerable level of residual vibration over any desired range of frequencies [25], [26]. One method for generating SI shapers uses evenly spaced points over the range of frequencies. At these distinct frequencies, residual vibration is constrained to below the tolerable level. For example, Figure 4 shows a case where residual vibrations are suppressed to below 5% over the range of 0.8 to 1.2 Hz.

III. Testing Apparatus

The container and camera in Figure 5 were mounted to an XY gantry. The gantry was driven by servomotors and

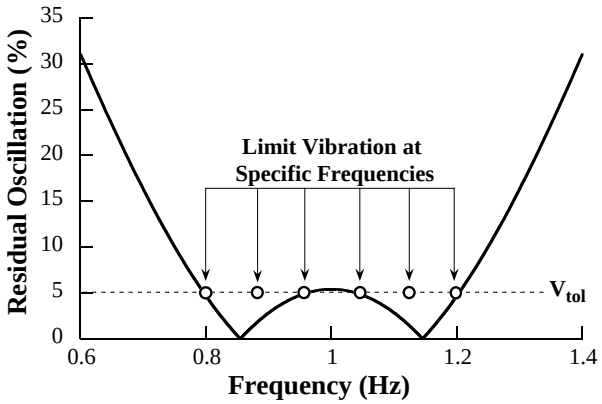

Figure 4. Specified Insensitivity (SI) Shaper Design Constraints

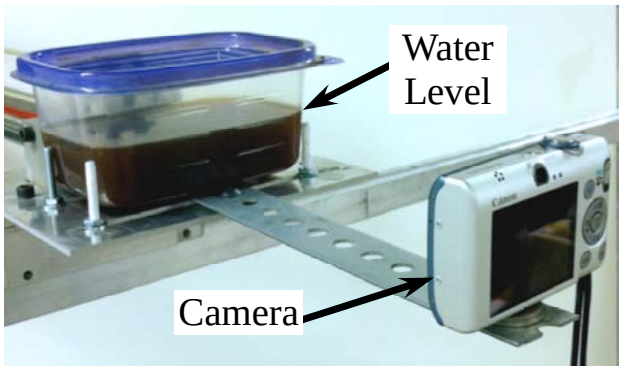

Figure 5. Testing Apparatus

controlled by a programmable logic controller [15]. The camera recorded the slosh inside the container.

The recorded video was downloaded to a computer for processing. Each frame was extracted from the video, as shown in Figure 6(a). The image was then thresholded, as shown in Figure 6(b). An outline of the water cross section was created by scanning the boundary between the white and black color, as shown in Figure 6(c). To measure slosh, the displacement of the rightmost point on the surface was recorded for each image. This point is denoted by the circle in Figure 6(c). The sampling period of the video was 16.7 ms with a resolution of approximately 0.5 mm.

A baseline case was selected. The container length, a, was 13 cm; the water depth, h, was 3.5 cm; and the natural frequency calculated from (1) was 12.78 rad/s. The container was moved, and the slosh was recorded. The estimated damping ratio and natural frequency were $\zeta = 0.008$ and $\omega = 12.5$ rad/s. The experimentally determined value and the estimated value from (1) differ by only 2.1%.

IV. Input Shaper Design

In order to intelligently design an input shaper, it is necessary to understand the system operating conditions. When moving a container of known dimensions, the primary concern is the liquid depth. With reference to Figure 1, there are three cases to consider. Case 1 is if the system frequency is always greater than the 95% line. Here, system frequency undergoes small changes and robustness may not

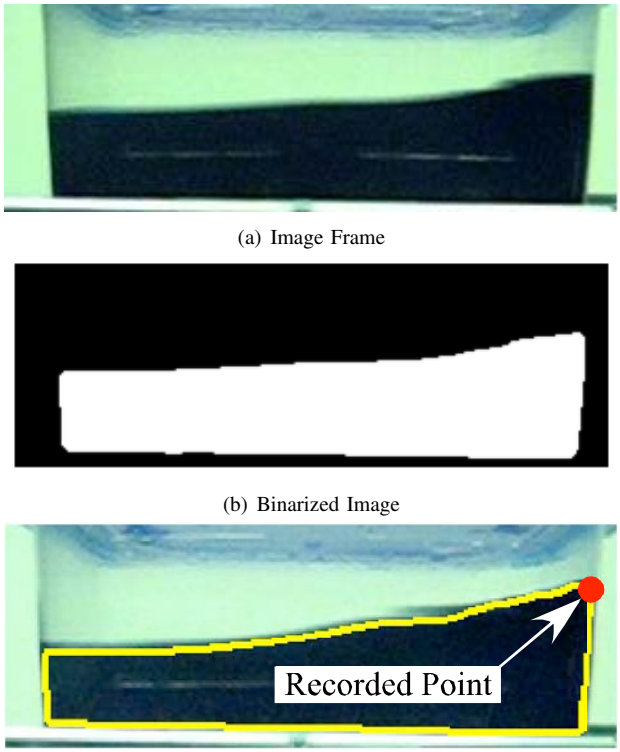

(a) Image Frame

(b) Binarized Image

(c) Boundary and Recorded Point

Figure 6. Data Processing

be a primary concern. Case 2 is if the nominal frequency is below the 95% line and the liquid depth is roughly constant. Then, the system frequency is also roughly constant, but moderate robustness may be desired for uncertainties. Case 3 is if the system frequency is below the 95% line and the liquid depth varies. Here, system frequency changes are large, and robustness is important. For this paper, case 3 is used to demonstrate slosh suppression by robust input shaping.

Three input shapers were evaluated in simulations and experimental testing. ZV and ZVD shapers were designed to suppress slosh for the baseline case. An SI shaper was designed to suppress slosh for liquid depths between 1 cm and 4.5 cm to a residual vibration level of 5%. Figure 7 shows this region and the corresponding frequencies. The upper bound was chosen to be near the top of the container. At the lower bound, the frequency changes significantly with liquid depth. The SI shaper that reduces slosh for these depths is 62% longer in duration than the ZVD shaper.

V. Simulations

Simulations of the slosh induced by unshaped and shaped commands for the baseline case are shown in Figure 8. In each simulation, the system was given a reference bang-coast-bang command with a four-second coast period. Two important pieces of data are seen in each simulation: the maximum transient deflection and the residual oscillation. The unshaped command in Figure 8(a) produces the greatest transient deflection. It is important to note that the maximum deflection caused by the unshaped command is dependent

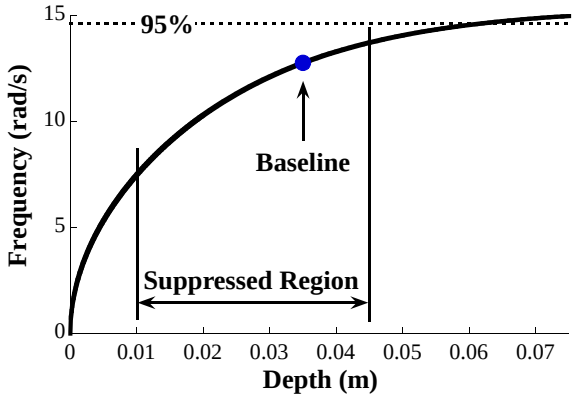

Figure 7. Frequencies Suppressed by SI Shaper

on the move distance and system frequency. In this case, the deceleration command slightly increases the amplitude of oscillation. The ZV-shaped command in Figure 8(b) reduces the transient deflection to 50% of that caused by the unshaped command. The ZVD-shaped command in Figure 8(c) further reduces the deflection to 25% at two peaks. The maximum deflection due to the ZV- and ZVD-shaped commands is not dependent on the move distance or system frequency for well-modeled systems. The SI-shaped command in Figure 8(d) causes a maximum deflection of only 19%. Although there are small residual oscillations, the maximum possible transient deflection induced by an SI-shaped bang-coast-bang command is 24% within the region of suppressed frequencies compared to 200% from an unshaped command.

The unshaped command in Figure 8(a) causes a residual oscillation amplitude of 74%. Both the ZV- and ZVD-shaped commands eliminate residual oscillations because the model is perfect. The SI-shaped command reduces residual oscillations to 2%. Residual oscillations due to the SI-shaped command have a slight dependence on move distance and system frequency.

In order to analyze robustness to parameter changes, Figure 9 shows the residual oscillation amplitude resulting from the three shaped commands over a range of system frequencies. Here, 100% residual oscillation is the amount of residual oscillation resulting from a step command. A line is drawn at 5% showing the acceptable level of residual oscillation. The ZV and ZVD shapers eliminate oscillation at the design frequency of 12.78 rad/s. The ZVD shaper provides more robustness to modeling errors than the ZV shaper with a larger range of suppressed frequencies below 5%. The SI shaper suppresses residual vibration to 5% between the frequencies of 7.50 rad/s and 16.20 rad/s. The appearance of the small residual oscillations in Figure 8(d) are also explained here. At a system frequency of 12.78 rad/s, the SI shaper is shown to have slightly greater than 0% residual oscillation amplitude.

VI. Experimental Results

Using a trapezoidal velocity as the reference command, the container was moved 50 cm in approximately 4 seconds. The ZV-, ZVD-, and SI-shaped commands were generated

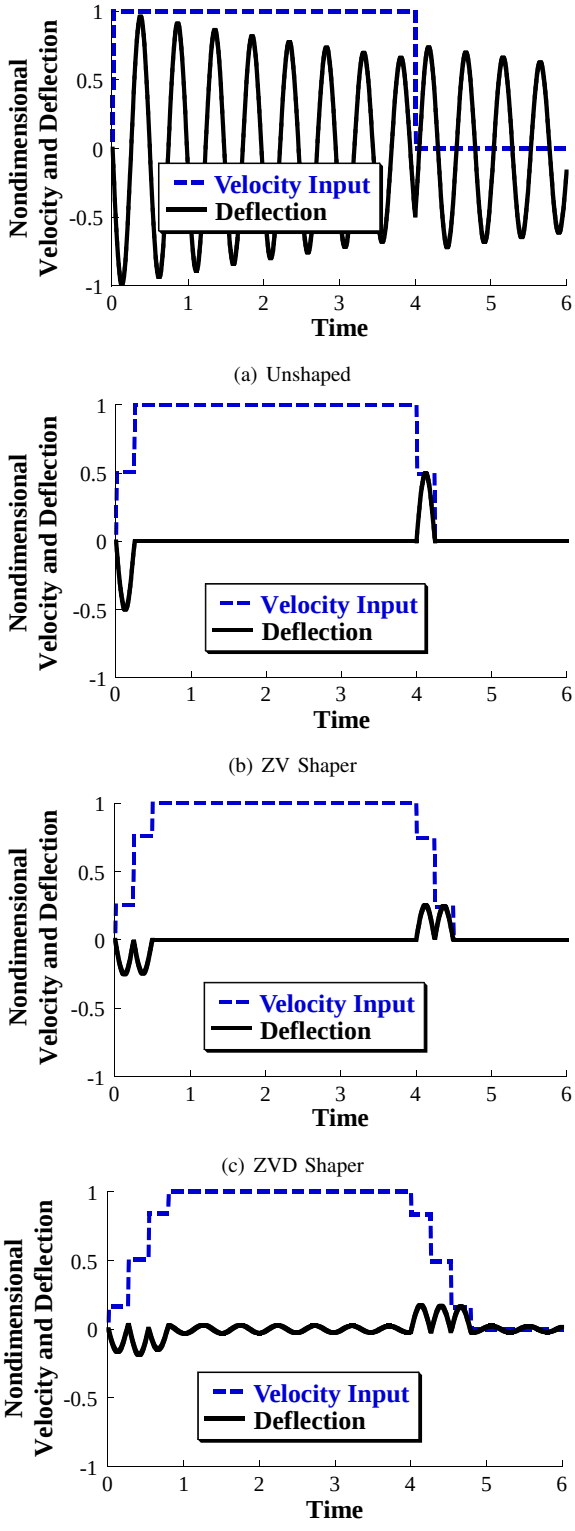

(a) Unshaped

(b) ZV Shaper

(c) ZVD Shaper

(d) SI Shaper

Figure 8. Simulated Slosh Response

from the reference command. During each test, transient and residual slosh were recorded. Two metrics were used to analyze the results: the maximum transient deflection, and the settling time defined as the time to reach 1.5 mm of residual oscillation.

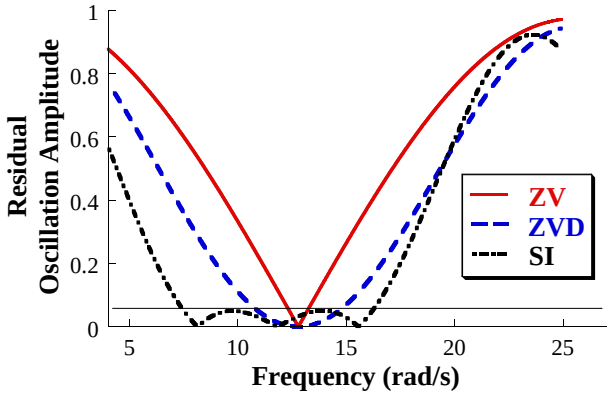

Figure 9. Sensitivity Curves for Input Shapers

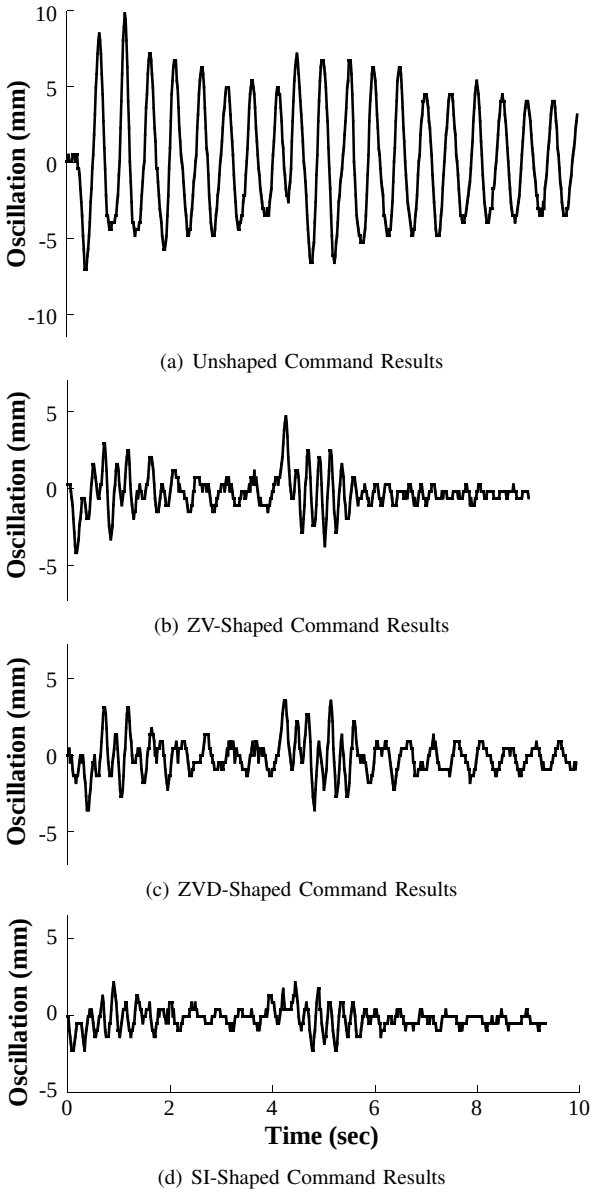

(a) Unshaped Command Results

(b) ZV-Shaped Command Results

(c) ZVD-Shaped Command Results

(d) SI-Shaped Command Results

Figure 10. Experimental Results for 3.5 cm Depth

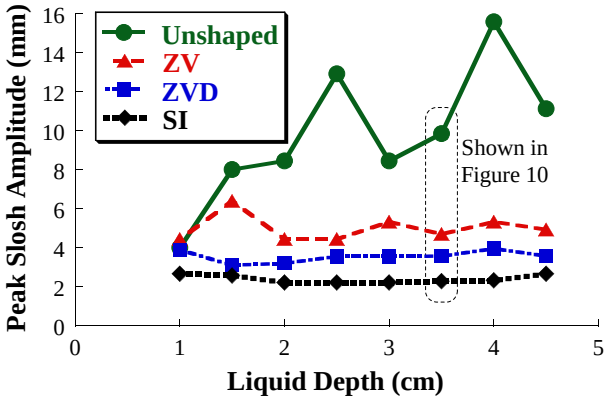

Figure 11. Peak Transient Slosh vs. Liquid Depth

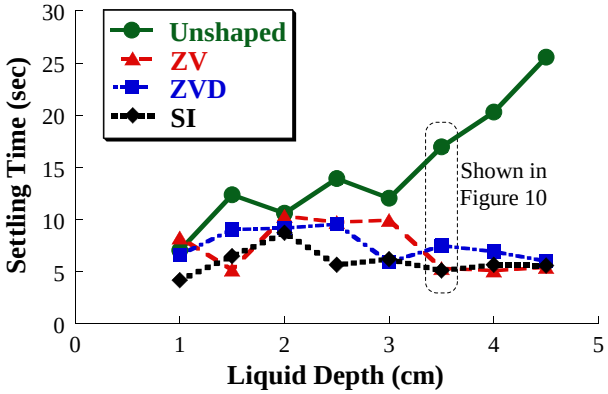

Figure 12. Settling Time vs. Liquid Depth

Figure 10 shows the slosh induced by the four commands with a liquid depth of 3.5 cm. Recall that this was the design point for the ZV and ZVD shapers. In each case, the initial acceleration induced slosh that partially damped out during the move. Four seconds later, the deceleration resulted in additional slosh. The peak transient slosh in the unshaped case of Figure 10(a) was 9.8 mm compared to an average of 3.5 mm for the shaped commands. The settling time for the unshaped case in Figure 10(a) was 17.0 seconds compared to an average of 6.0 seconds for the shaped commands. For this particular case, the ZV command suppressed residual slosh slightly better than the ZVD command, as shown in Figures 10(b) and 10(c). However, the ZVD command resulted in lower peak transient slosh than the ZV command, as expected. The SI command, shown in Figure 10(d), suppressed residual slosh better than the other shaped commands, with the added benefit of lower peak transient slosh.

Figure 11 shows the peak transient slosh amplitude for the four commands at several liquid depths. These results correlate with the deflections predicted by Figure 8. The unshaped command had the greatest slosh amplitude for nearly all cases with an average of 9.8 mm. The variance at different liquid depths was due to the dependence on system frequency. The ZV, ZVD and SI commands significantly decreased the peak transient slosh amplitude, with averages of 5.0 mm, 3.6 mm, and 2.4 mm, respectively.

Figure 12 shows the settling time for the four move

commands at each liquid depth. For all cases except for the ZV-shaped 1 cm test, the unshaped command had a settling time greater than the shaped commands and an average settling time of 14.8 s. The unshaped command had a greater settling time at greater liquid depths due to the dependence of residual oscillations on system frequency. The ZV and ZVD command averaged 7.4 s and 7.5 s, respectively, to settle. The SI shaper reduced settling time for the majority of the cases with an average of 5.9 s.

VII. Conclusions

The slosh in a rectangular container of liquid was reduced with Zero Vibration, Zero Vibration and Derivative, and Specified Insensitivity (SI) input shapers. Simulations showed that input-shaped commands can significantly reduce peak transient and residual slosh. Additionally, robust input shaping was shown to suppress oscillation of the first mode of slosh over a range of system frequencies. Experiments verified the key results predicted by the simulations. The robust SI shaper resulted in the lowest peak transient slosh and the fastest average settling time over a range of liquid depths.

Acknowledgment

The authors would like to thank Siemens Industrial Automation, British Petroleum, and the Manufacturing Research Center at Georgia Tech for their support of this work.

References

[1] Ameen Aboel-Hassan, Mustafa Arafa, and Ashraf Nassef. Design and optimization of input shapers for liquid slosh suppression. *Journal of Sound and Vibration*, 320:1–15, 2009.

[2] H. Norman Abramson. The dynamic behavior of liquids in moving containers. Technical Report SP-106, NASA, 1966.

[3] Tankut Acarman and Umit Ozguner. Rollover prevention for heavy trucks using frequency shaped sliding mode control. *Vehicle System Dynamics*, 44(10):737 – 762, 2006.

[4] B. Bandyopadhyay, P.S. Gandhi, and Shailaja Kurode. Sliding mode observer based sliding mode controller for slosh-free motion through pid scheme. *IEEE Transactions on Industrial Electronics*, 56(9):3432 –3442, September 2009.

[5] SJ Chen, B Hein, and H Worn. Using acceleration compensation to reduce liquid surface oscillation during a high speed transfer. In *IEEE International Conference on Robotics and Automation*, pages 2951–2956, April 2007.

[6] Franklin T. Dodge. The new 'Dynamic behavior of liquids in moving containers'. Technical report, Southwest Research Institute, 2000.

[7] John T. Feddema, Clark R. Dohrmann, Gordon G. Parker, Rush D. Robinett, and Dan J. Romero, Vincente J.and Schmitt. Control for slosh-free motion of an open container. *IEEE Control Systems*, pages 29–36, 1997.

[8] Prasanna S. Gandhi, Keyur B. Joshi, and N. Ananthkrishnan. Design and development of a novel 2DOF actuation slosh rig. *Journal of Dynamic Systems, Measurement, and Control*, 131(1):011006–1–011006–9, 2009.

[9] M. Grundelius and B. Bernhardsson. Constrained iterative learning control of liquid slosh in an industrial packaging machine. In *39th IEEE Conference on Decision and Control*, volume 5, pages 4544 –4549, 2000.

[10] Masafumi Hamaguchi, Yu Yoshida, Tomohiko Kihara, and Takao Taniguchi. Path design and trace control of a wheeled mobile robot to damp liquid sloshing in a cylindrical container. In *IEEE International Conference on Mechatronics and Automation*, volume 4, pages 1959 – 1964, July-1 Aug. 2005.

[11] F. Hara. Refined active control of sloshing by intermittent gas-bubble injection. In *First International Conference on Motion and Vibration Control*, pages 1104–1109, September 1992.

[12] R. A. Ibrahim, V. N. Pilipchuk, and T. Ikeda. Recent advances in liquid sloshing dynamics. *Applied Mechanics Reviews*, 54(2), 2001.

[13] Y Komoguchi, M Kunieda, and K Yano. Liquid handling control for service robot by hybrid shape approach. In *SICE Annual Conference*, pages 1737–1740, August 2008.

[14] Shailaja Kurode, B. Bandyopadhyay, and P.S. Gandhi. Sliding mode control for slosh-free motion of a container using partial feedback linearization. In *International Workshop on variable Structure Systems*, pages 367 –372, June 2008.

[15] Jason Lawrence and William Singhose. Design of minicrane for education and research. In *6th Int. Conference on Research and Education in Mechatronics*, Annecy, France, 2005.

[16] K. Muto, Y. Kasai, and M. Nakahara. Experimental tests for suppression effects of water restraint plates in sloshing of a water pool. *Journal of Pressure Vessel Technology*, 110:240–246, 1988.

[17] Y. Noda, K. Yano, S Horihata, and K. Terashima. Sloshing suppression control during liquid container transfer involving dynamic tilting using Wigner distribution analysis. In *43rd IEEE Conference on Decision and Control*, volume 3, pages 3045 – 3052 Vol.3, December 2004.

[18] CS Oh, BC Sun, YK Park, and WR Roh. Sloshing analysis using ground experimental apparatus. In *International Conference on Control, Automation and Systems*, pages 2203–2207, October 14-17 2008.

[19] Lee D. Perterson, Edward F. Crawley, and R. John Hansman. Nonlinear fluid slosh coupled to the dynamics of spacecraft. *AIAA Journal*, 27(9):1230–1240, 1989.

[20] Naiming Qi, Kai Dong, Xianlu Wang, and Yunqian Li. Spacecraft propellant sloshing suppression using input shaping technique. pages 162 –166, Feb. 2009.

[21] James R. Roberts, Eduardo R. Basurto, and Pei-Ying Chen. Slosh design handbook I. Technical Report CR-406, NASA, 1966.

[22] Neil C. Singer and Warren P. Seering. Preshaping command inputs to reduce system vibration. *J. of Dynamic Sys., Measurement, and Control*, 112:76–82, 1990.

[23] W Singhose. Command shaping for flexible systems: A review of the first 50 years. *International Journal of Precision Engineering and Manufacturing*, 10(4):153–168, 2009.

[24] W. Singhose and W. Seering. *Command Generation for Dynamic Systems*. www.lulu.com/content/621219. 978-0-9842210-0-4, 2010.

[25] William Singhose, Dooroo Kim, and Michael Kenison. Input shaping control of double-pendulum bridge crane oscillations. *ASME J. of Dynamic Systems, Measurement, and Control*, 130(034504), May 2008.

[26] William Singhose, Warren Seering, and Neil Singer. Input shaping for vibration reduction with specified insensitivity to modeling errors. In *Japan-USA Sym. on Flexible Automation*, volume 1, pages 307–13, Boston, MA, 1996.

[27] Hebertt Sira-Ramirez and Michel Fliess. A flatness based generalized PI control approach to liquid sloshing regulation in a moving container. In *American Control Conference*, volume 4, pages 2909 – 2914, 2002.

[28] O. J. M. Smith. *Feedback Control Systems*. McGraw-Hill Book Co., Inc., New York, 1958.

[29] Kazuhiko Terashima, Masafumi Hamaguchi, and Kazuto Yano. Modeling and input shaping control of liquid vibration for an automatic pouring system. In *35th IEEE Conference on Decision and Control*, pages 4844–4850, 1996.

[30] Kazuhiko Terashima and Gunther Schmidt. Motion control of a cart-based container considering suppression of liquid oscillations. In *IEEE International Symposium on Industrial Electronics*, pages 275 –280, May 1994.

[31] Kazuhiko Terashima and Ken'ichi Yano. Sloshing analysis and suppression control of tilting-type automatic pouring machine. *Control Engineering Practice*, 9(6):607 – 620, 2001.

[32] Ravinder Venugopal and Dennis S. Bernstein. State space modeling and active control of slosh. In *IEEE International Conference on Control Applications*, pages 1072 –1077, September 1996.

[33] K Yano and K Terashima. Sloshing suppresion control of liquid transfer systems considering a 3-d transfer path. *IEEE/ASME Transactions on Mechatronics*, 20(1):8–16, 2005.

[34] K. Yano, T. Toda, and K. Terashima. Sloshing suppression control of automatic pouring robot by hybrid shape approach. In *40th IEEE Conference on Decision and Control*, volume 2, pages 1328 –1333, 2001.

[35] Ken'ichi Yano and Kazuhiko Terashima. Robust liquid container transfer control for complete sloshing suppression. *IEEE Transactions on Control Systems Technology*, 9(3):483 –493, May 2001.